Chemistry & Biodiversity

CHEMISTRY & BIODIVERSITY

RESEARCH ARTICLE

Ligustrum sinense Lour.: Essential Oil Compositions, Biological Activities, and In Silico Studies—A First Record

Ninh The Son[1] | Phan Hong Minh[2] | Huynh Thi Ngoc Ni[3] | Nguyen Ngoc Linh[4] | Nguyen Thi Kim Thanh[5] | Le The Hoai[6] | Nguyen Thi Thoa[6] | Nguyen Xuan Ha[1] | Ty Viet Pham[7]

[1]Institute of Chemistry, Vietnam Academy of Science and Technology (VAST), Hanoi, Vietnam | [2]University of Medicine and Pharmacy, Vietnam National University (VNU), Hanoi, Vietnam | [3]Faculty of Education, Ha Tinh University, Ha Tinh, Vietnam | [4]Institute of Medicine and Pharmacy, Thanh Do University, Hanoi, Vietnam | [5]Faculty of Biology, University of Science, VNU, Hanoi, Vietnam | [6]Faculty of Chemical Technology, Hanoi University of Industry, Hanoi, Vietnam | [7]Faculty of Chemistry, University of Education, Hue University, Hue, Vietnam

Correspondence: Ty Viet Pham (phamvietty@hueuni.edu.vn)

Received: 19 July 2025 | **Revised:** 10 November 2025 | **Accepted:** 26 November 2025

Keywords: biological activity | essential oil | *Ligustrum sinense* | molecular docking | toxicity prediction

ABSTRACT

The current study first describes the gas chromatography–mass spectrometry (GC–MS) chemical analysis of essential oils from *Ligustrum sinense* (the family Oleaceae). Linalool (5.0%), *cis*-phytol (5.1%), methyl salicylate (5.4%), and germacrene B (7.9%) dominated in the twig essential oil. Methyl salicylate (5.5%), linalool (7.4%), and germacrene B (14.2%) were the major compounds in the leaf essential oil, whereas *cis*-phytol (5.8%), linalool (6.9%), and germacrene B (17.2%) were characteristic compounds in the flower essential oil. *L. sinense* essential oils (IC_{50} 208.09–245.39 μg/mL) are comparable to the standard acarbose (IC_{50} 241.76 μg/mL) in α-glucosidase inhibitory activity. The leaf essential oil (IC_{50} 4.51 μg/mL) is much better than the standard ascorbic acid (IC_{50} 13.64 μg/mL) in DPPH radical scavenging. The studied essential oils also exhibited xanthine oxidase inhibitory, anti-inflammatory, protein tyrosine phosphatase 1B inhibitory, and antimicrobial activities. Molecular docking targeting human aldose reductase (PDB ID: 3WY1) revealed strong binding affinities with the major compounds. Germacrene B showed the highest affinity (−6.637 kcal/mol), followed by *cis*-phytol (−5.729 kcal/mol), forming stable hydrophobic interactions within the enzyme's active site. Toxicity predictions indicated that germacrene B, *cis*-phytol, and linalool are relatively safe (toxicity class 5).

1 | Introduction

Ligustrum sinense Lour., commonly referred to as "Chinese privet" or "Ram tau" in Vietnamese, is a deciduous to semievergreen shrub indigenous to China, Taiwan, and Vietnam [1]. With its vigorous growth and capacity to outcompete native vegetation, this species has also been widely introduced to various parts of the world, including the Eastern and Southern United States [1].

In traditional Chinese medicine, *L. sinense* has been utilized for its diverse pharmacological activities, particularly antioxidant, anti-inflammatory, hepatoprotective, and immunomodulatory effects [2, 3]. Phytochemical separations have identified various bioactive constituents, including secoiridoids like oleuropein, flavonoids, lignans, and triterpenoids [2, 3]. Extracts derived from its leaves, barks, and fruits have demonstrated potential therapeutic value in various experimental models, exhibiting antimicrobial, anticancer, and neuroprotective properties [2–5].

Essential oils derived from plants of the genus *Ligustrum* have garnered increasing scientific interest due to their diverse chemical compositions and potential biological activities. Various *Ligustrum* species, such as *L. lucidum* and *L. japonicum*, have been traditionally used in Asian medicine. Therefore, recent studies have focused on analyzing their volatile constituents through gas chromatography–mass spectrometry (GC–MS)

analysis. Chemical compositions of *Ligustrum* essential oils may vary depending on species, geographical origin, extraction method, and plant part. *Ligustrum* essential oils contained monoterpene hydrocarbons, sesquiterpene hydrocarbons and their oxygenated derivatives, and aromatic compounds as major constituents. Compounds, such as linalool, α-pinene, β-caryophyllene, and several non-terpenoids, have been frequently reported [6–10].

L. japonicum leaf essential oil was dominated by germacrene D (40.50%), α-pinene (13.63%), (−)-β-elemene (6.42%), β-caryophyllene (5.73%), and δ-cadinene (5.47%) [6]. Linalool ranged from 48.34% to 79.25% in the insecticidal essential oils of *Ligustrum robust* leaves and buds [7]. Antibacterial properties of *Ligustrum obtusifolium* flower essential oil may be due to the predominance of non-terpenic compounds, such as butyl hydroxyl anisole (12.53%) and 2-allybenzyl phenyl sulfide (12.10%) [8]. In the same manner, antibacterial features of *Ligustrum compactum* flower essential oil may be attributed to 2-phenylethanol (61.660%), linalool (8.853%), benzyl alcohol (7.972%), and guaiacol (4.114%) [9]. *L. lucidum* flower essential oil with food-borne pathogenic bacterial effects was characterized by styrene glycol (26.63%) and formic acid (14.58%) [10].

The current research aims to offer a chemical analysis using the GC–MS to identify chemical profiles of essential oils obtained from Vietnamese *L. sinense* twigs, leaves, and flowers. The studied samples have been evaluated for their usefulness as promising agents in antioxidant, xanthine oxide (XO) inhibition, anti-inflammation, anti-diabetes, and antibacterial activity. In silico approaches are also performed to highlight the great role of the major compounds with potential biological effects and their toxicological values.

2 | Results and Discussion

2.1 | Phytochemical Analysis

Hydro-distillation of the fresh twigs yielded a yellowish essential oil with a yield of 0.34% (v/w). On the basis of GC–MS analysis, a total of 88 compounds were identified, accounting for 99.1% of the total composition (Table 1 and Figure S1). The twig essential oil was dominated by non-terpenic compounds (28.1%) and sesquiterpene hydrocarbons (27.5%), followed by oxygenated sesquiterpenes (18.0%), oxygenated monoterpenes (17.7%), oxygenated diterpenes (5.5%), and monoterpene hydrocarbons (2.3%). The major constituents of essential oil included germacrene B (7.9%), methyl salicylate (5.4%), *cis*-phytol (5.1%), and linalool (5.0%). Several other compounds were present in amounts greater than 1.0%, for example, (*E*)-β-damascenone (4.3%), benzaldehyde and γ-elemene (3.8% each), borneol and *n*-tetradecanol (3.0% each), valerianol (2.4%), *trans*-sesquisabinene hydrate (2.1%), and juniper camphor (2.0%).

The extraction of the fresh leaves also produced a yellowish essential oil with a yield of 0.37% v/w. A list of 83 identified compounds, which correspond to 98.2%, is outlined in Table 1 and Figure S2. The leaf essential oil was characterized by sesquiterpene hydrocarbons (41.9%), non-terpenic compounds (23.2%), and oxygenated monoterpenes (18.2%). In the meantime, other classes included oxygenated sesquiterpenes (10.2%), monoterpene hydrocarbons (3.5%), and oxygenated diterpenes (1.2%). The principal compounds were germacrene B (14.2%), linalool (7.4%), and methyl salicylate (5.5%). Several other compounds were also noteworthy, each exceeding 1.0%; for example, *n*-hexanol (4.7%), (*E*)-β-damascenone (4.3%), γ-elemene (3.7%), benzaldehyde (2.7%), α-terpineol (2.6%), β-pinene (2.4%), (2*Z*)-hexenol (2.3%), and δ-cadinene (2.0%).

In another case, a yellowish essential oil (0.26% v/w) was obtained from hydro-distillation of the fresh flowers. For Table 1 and Figure S3, 80 compounds were identified, which represented 99.2%. Sesquiterpene hydrocarbons reached the highest proportion of 51.3%, whereas oxygenated derivatives of monoterpenes and sesquiterpenes had the same rate of 13.8%. The other groups comprised non-terpenic compounds (13.5%), oxygenated diterpenes (6.3%), and monoterpene hydrocarbons (0.5%). The flower essential oil was associated with the appearance of germacrene B (17.2%), linalool (6.9%), and *cis*-phytol (5.8%). The sample is also noted with the presence of other significant compounds, for example, γ-elemene (3.5%), (*E*)-caryophyllene (3.3%), germacrene D (3.2%), benzaldehyde and (*E*)-β-damascenone (3.1%, each), δ-cadinene (2.6%), α-selinene (2.5%), (*E*)-β-farnesene and valerianol (2.1%, each), and 10-epi-*cis*-dracunculifoliol (1.8%).

All three essential oils were dominated by sesquiterpene hydrocarbons, with the highest percentage observed in the flowers (51.3%), followed by the leaves (41.9%) and twigs (27.5%). Oxygenated monoterpenes were the second most abundant class in the twigs (17.7%) and leaves (18.2%), but relatively lower in the flowers (13.8%). Remarkably, non-terpenic compounds constituted a major portion in the twigs (28.1%), whereas this proportion decreased in the leaves (23.2%) and was lowest in flowers (13.5%). Regarding major compounds (≥5%), germacrene B was the most dominant agent in all the samples, including the flowers (17.2%), leaves (14.2%), and twigs (7.9%). Linalool and *cis*-phytol were also prominent in all three oils, with linalool content being highest in the leaves (7.4%) and *cis*-phytol being highest in the flowers (5.8%). Other major constituents included methyl salicylate in twigs (5.4%) and leaves (5.5%). In terms of compound occurrence, certain compounds were exclusive or notably abundant in specific organs. For example, (*2Z*)-hexenol and pinocarvone were detected only in the leaves, whereas *n*-heneicosane and palmitic acid appeared uniquely in the twigs. Some compounds, such as bicycloelemene and myristicin, were only found in the flowers. This reveals organ-specific biosynthesis or accumulation of secondary metabolites. Collectively, the variations in chemical compounds suggest functional differentiation in secondary metabolite production among *L. sinense* twigs, leaves, and flowers, potentially reflecting their ecological roles or physiological states.

As mentioned above, monoterpenes, sesquiterpenes, and their oxygenated derivatives, as well as non-terpenic compounds, were characteristic compounds of *Ligustrum* essential oils [6–10]. As an example, germacrene D is marked in *L. japonicum* leaf essential oil up to 40.50% [6]. Linalool ranged from 48.34% to 79.25% in essential oils of *L. robust* leaves and buds [7]. Hydroxyl anisole and 2-allybenzyl phenyl sulfide were non-terpenic compounds in *L. obtusifolium* flower essential oil, with about 12%–13%, whereas 2-phenylethanol (61.660%) was overwhelming in *L. compactum*

TABLE 1 | Chemical compositions in *Ligustrum sinense* essential oils.

RT	Compounds	RI_E	RI_L	Twigs	Leaves	Flowers	Classification
3.82	*n*-Hexanal	800	801	0.3			NT
4.47	Furfural	828	828	0.3			NT
4.91	(2*E*)-Hexenal	848	846	0.2	0.8		NT
4.98	(3*Z*)-Hexenol	851	850	0.5	1.4	0.2	NT
5.19	(2*Z*)-Hexenol	861	859		2.3		NT
5.26	*n*-Hexanol	864	863	0.9	4.7	0.3	NT
8.03	Benzaldehyde	958	952	3.8	2.7	3.1	NT
8.47	Sabinene	971	969		0.5		MH
8.68	*β*-Pinene	977	974	0.6	2.4	0.3	MH
9.87	*δ*-3-Carene	1010	1008		0.3		MH
9.89	(2*E*,4*E*)-Heptadienal	1010	1005	0.4			NT
10.61	*β*-Phellandrene	1028	1025	0.2			MH
11.19	Benzeneacetaldehyde	1042	1036	1.0	0.2	0.5	NT
12.23	(2*E*)-Octen-1-ol	1067	1060		0.2		NT
12.36	*n*-Octanol	1070	1063	0.6	0.8	0.2	NT
12.44	*cis*-Linalool oxide (furanoid)	1072	1067	1.0	0.3		OM
12.60	Benzyl formate	1076	1071	0.5	0.2		NT
13.11	Terpinolene	1088	1086	1.5	0.3	0.2	MH
13.59	Linalool	1100	1095	**5.0**	**7.4**	**6.9**	OM
13.77	*n*-Nonanal	1104	1100	0.5	0.3	0.2	NT
14.09	*cis*-Rose oxide	1111	1106		0.2		OM
16.24	(2*E*)-Nonen-1-al	1159	1157	0.2			NT
16.54	Pinocarvone	1166	1160		0.2		OM
16.56	Borneol	1166	1165	3.0	0.6	0.3	OM
17.05	Terpinen-4-ol	1177	1174	0.7			OM
17.67	*α*-Terpineol	1191	1186	1.4	2.6	1.5	OM
17.81	Methyl salicylate	1194	1190	**5.4**	**5.5**	1.6	NT
18.56	Berbenone	1211	1205	1.0	0.8	0.5	OM
18.75	*trans*-Carveol	1215	1215		0.2		OM
19.34	Hydrocinnamyl alcohol	1229	1224	0.6	0.7	0.6	NT
20.51	Geraniol	1255	1249	0.9	1.3	1.3	OM
21.28	(*E*)-Cinnamaldehyde	1272	1267		0.4		NT
22.08	Bornyl acetate	1290	1284		0.3		OM
23.22	4-Hydroxy-cryptone	1316	1314	0.5		0.1	OM
24.16	Bicycloelemene	1338	1338			0.1	SH
25.01	Eugenol	1358	1356	0.4	0.3		NT
25.85	*α*-Ylangene	1377	1373		0.2	0.3	SH
26.21	(*E*)-*β*-Damascenone	1386	1383	4.3	4.3	3.1	OM
26.36	*β*-Bourbonene	1389	1387	0.4	0.5	0.3	SH
26.53	*β*-Elemene	1393	1389	0.8	1.4	1.7	SH
27.50	*α*-Gurjunene	1416	1409	0.5	0.5	0.3	SH
27.70	(*E*)-Caryophyllene	1421	1417	1.0	2.8	3.3	SH
27.95	D-8-Hydroxycarvotanacetone	1427	1424		0.1	0.1	OS

(Continues)

TABLE 1 | (Continued)

RT	Compounds	RI_E	RI_L	Twigs	Leaves	Flowers	Classification
28.06	β-Copaene	1430	1430	0.3	0.4	0.4	SH
28.27	γ-Elemene	1435	1434	3.8	3.7	3.5	SH
28.48	Aromadendrene	1440	1439	0.2	1.3	1.4	SH
28.68	6,9-Guaiadiene	1445	1442	0.3	1.7	1.8	SH
28.90	(*E*)-Isoeugenol	1450	1448	0.2			NT
29.04	Neryl propanoate	1453	1452	0.7			NT
29.05	α-Humulene	1454	1452		0.6	1.7	SH
29.12	(*E*)-β-Farnesene	1455	1454	0.8	0.8	2.1	SH
29.41	allo-Aromadendrene	1463	1458	0.4	0.4	0.6	SH
29.58	Dehydroaromadendrane	1467	1460	0.7	0.4	0.4	SH
29.93	α-Macrocarpene	1473	1470		0.1		SH
30.02	β-Chamigrene	1478	1476	0.5	0.5	0.7	SH
30.25	Germacrene D	1483	1480	1.9	2.3	3.2	SH
30.45	β-Selinene	1488	1489	1.3	0.9	1.2	SH
30.66	γ-Amorphene	1493	1490	0.5	0.8	0.9	SH
30.83	α-Selinene	1497	1498	1.0	1.1	2.5	SH
30.85	Bicyclogermacrene	1499	1500		1.6		SH
31.03	α-Muurolene	1502	1500	0.5	0.4	0.6	SH
31.31	(*E*,*E*)-α-Farnesene	1509	1505	0.9	1.0	1.4	SH
31.43	α-Bulnesene	1512	1509	0.4	0.3	0.3	SH
31.58	δ-Amorphene	1516	1511	0.4	0.5	0.7	SH
31.73	Myristicin	1520	1517			0.2	NT
31.96	δ-Cadinene	1526	1522	1.6	2.0	2.6	SH
32.42	α-Cadinene	1538	1537	0.4	0.5	0.7	SH
32.53	10-epi-*cis*-Dracunculifoliol	1540	1540	1.0		1.8	OS
32.70	α-Calacorene	1544	1544	1.0	1.0	1.4	SH
33.04	Elemol	1553	1548		0.2		OS
33.31	Germacrene B	1560	1559	**7.9**	**14.2**	**17.2**	SH
33.50	(*E*)-Nerolidol	1565	1561	1.4	0.8	1.2	OS
34.10	*trans*-Sesquisabinene hydrate	1580	1577	2.1	1.0		OS
34.36	Caryophyllene oxide	1587	1582	0.7	0.4	0.5	OS
34.47	Globulol	1590	1590		0.2		OS
34.67	Viridiflorol	1595	1592	0.4		0.2	OS
34.87	Guaiol	1600	1600	0.5		0.2	OS
35.66	2,(7*Z*)-Bisaboladien-4-ol	1621	1618	0.4	0.4	0.4	OS
36.05	1-epi-Cubenol	1631	1627	0.3	0.3	0.3	OS
36.18	γ-Eudesmol	1635	1630	0.4	0.4	0.4	OS
36.42	*allo*-Aromadendrene epoxide	1641	1639	0.3			OS
36.56	Torreyol	1645	1644	1.5	1.5	1.6	OS
36.72	β-Eudesmol	1649	1649	0.2	0.3	0.2	OS
36.84	Cedr-8(15)-en-10-ol	1653	1650	0.9		0.3	OS
36.94	Pogostol	1655	1651		0.3	0.2	OS
37.04	Valerianol	1658	1656	2.4	1.7	2.1	OS

(Continues)

TABLE 1 | (Continued)

RT	Compounds	RI_E	RI_L	Twigs	Leaves	Flowers	Classification
37.17	Allohimachalol	1661	1661	0.3			OS
37.33	14-Hydroxy-(*Z*)-caryophyllene	1666	1666	0.2			OS
37.49	Citronellyl tiglate	1670	1666	1.0	0.6	1.1	NT
37.65	Bulnesol	1674	1670	0.4	0.3	0.4	OS
37.81	*n*-Tetradecanol	1679	1671	3.0	0.5	1.2	NT
37.92	Khusinol	1682	1679	0.3			OS
38.07	epi-*α*-Bisabolol	1686	1683	0.3		0.2	OS
38.58	Juniper camphor	1699	1700	2.0	1.4	1.6	OS
38.80	Mayurone	1706	1703			0.3	OS
39.14	Cedroxyde	1715	1713	0.9	0.5	0.9	OS
39.35	(2*Z*,6*E*)-Farnesol	1721	1722	0.8	0.4	0.5	OS
39.45	(2*Z*,6*E*)-Farnesol	1724	1722			0.2	OS
39.71	iso-Longifolol	1731	1728			0.3	OS
41.13	*n*-Pentadecanol	1771	1773	1.0	0.4	0.9	NT
41.45	14-Hydroxy-*α*-muurolene	1780	1779	0.3			OS
43.72	Isoamyl dodecanoate	1846	1844	0.8	0.4	0.8	NT
47.62	Palmitic acid	1964	1959	1.5		0.5	NT
49.74	(6*Z*,10*E*)-Pseudo phytol	2032	2030	0.4	0.2	0.5	OD
51.88	*n*-Heneicosane	2101	2100	1.1		0.3	NT
52.31	*cis*-Phytol	2115	2113	**5.1**	1.0	**5.8**	OD
53.18	Palmitaldehyde, diallyl acetal	2145	2136	0.3		0.3	NT
54.63	1-Docosene	2194	2189		0.2	0.3	NT
57.70	*n*-Tricosane	2301	2300	1.9	0.4	0.9	NT
63.11	*n*-Pentacosane	2502	2500	0.5	0.2	0.2	NT
70.28	*n*-Heptacosane	2703	2700	0.5		0.1	NT
	Total			99.1	98.2	99.2	
	Monoterpene hydrocarbons (MH)			2.3	3.5	0.5	
	Oxygenated monoterpenes (OM)			17.7	18.2	13.8	
	Sesquiterpene hydrocarbons (SH)			27.5	41.9	51.3	
	Oxygenated sesquiterpenes (OS)			18.0	10.2	13.8	
	Oxygenated diterpenes (OD)			5.5	1.2	6.3	
	Non-terpenic compounds (NT)			28.1	23.2	13.5	

Note: Bold—major compound (≥5%).

Abbreviations: RI_E, experimental retention indices; RI_L, literature retention indices; RT, retention time.

flower essential oil [8, 9]. Essential oil from *L. lucidum* flowers was accompanied by styrene glycol (26.63%) and formic acid (14.58%) [10]. However, this is the first record in a chemical profile of *L. sinense* essential oils.

2.2 | Biological Activities

2.2.1 | Antioxidative Activity

The antioxidant activity of *L. sinense* essential oils was assessed using the DPPH free radical scavenging model at 32–512 μg/mL. At the highest tested concentration of 512 μg/mL, the leaf essential oil showed the strongest scavenging activity, achieving 91.45% ± 0.97%, and gradually decreased to 80.19% ± 1.11% (256 μg/mL), 75.50% ± 0.84% (128 μg/mL), 65.17% ± 0.76% (64 μg/mL), and 23.18% ± 0.68% (32 μg/mL) (Figure 1). This reflects a consistent and potent dose–response relationship, resulting in high antioxidant efficacy with a low IC_{50} value of 4.51 ± 0.03 μg/mL, which was better than that of the standard ascorbic acid (IC_{50} 13.64 ± 0.02 μg/mL) (Table 2). It might be due to its high contents of linalool, methyl salicylate, and *cis*-phytol.

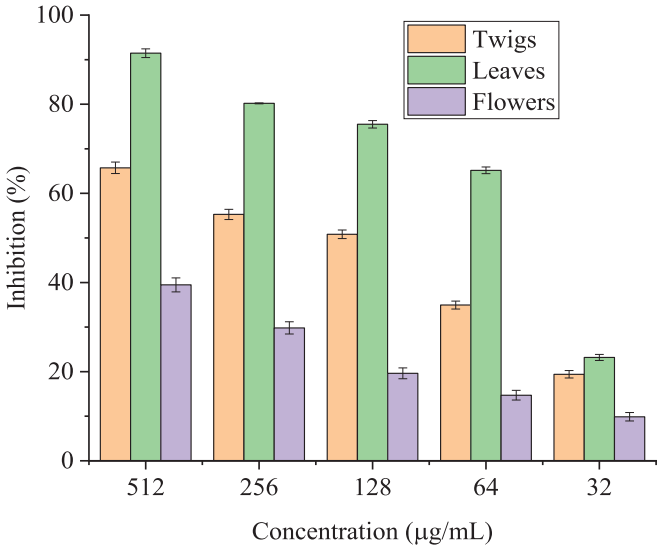

FIGURE 1 | The DPPH radical scavenging of *Ligustrum sinense* essential oils. Mean ± SD, n value = 3, $p < 0.05$ versus the non-treated group (0% inhibition).

The twig essential oil also possessed a dose-dependent response, but with lower potency: the inhibition decreased from 65.73% ± 1.29% at 512 μg/mL to 19.41% ± 0.83% at 32 μg/mL. By this means, the IC_{50} value was recorded to be 201.64 ± 0.05 μg/mL, suggesting weak antioxidant activity. The flower essential oil did not show activity. Its inhibition ranged from 9.88% ± 0.94% at 32 μg/mL to 39.47% ± 1.56% at 512 μg/mL, and its IC_{50} > 512 μg/mL.

Previously, essential oil from *L. compactum* flowers has been documented to quench DPPH and ABTS radicals with IC_{50} values of 83.28 ± 6.83 and 268.11 ± 3.21 μg/mL, respectively [9]. The aqueous extract of *Ligustrum robustum* leaves could dose-dependently exhibit inhibitions of superoxide radicals and lipid peroxidation, which were comparable to the potencies of green, oolong, and black teas [11]. These findings suggest that *L. sinense* leaf essential oils and other related species are the most promising source for natural antioxidant development.

2.2.2 | XO Activity

The XO inhibitory effects of *L. sinense* essential oils were evaluated at different concentrations of 0.8–100 μg/mL. All samples showed a concentration-dependent increase in XO inhibition. At 100 μg/mL, the leaf essential oil exhibited the highest inhibition of 92.04% ± 1.09%, whereas the twig and flower essential oils showed moderate effects at 37.41% ± 1.30% and 33.22% ± 1.88%, respectively (Figure S4). As concentration decreased, the inhibitory capacity of all samples dropped significantly. For instance, at 20 μg/mL, the leaf essential oil inhibition dropped to 13.97% ± 1.36%, and the twig and flower essential oils to 20.47% ± 1.06% and 22.91% ± 1.37%, respectively. At the lowest tested concentration of 0.8 μg/mL, *L. sinense* essential oils showed weak activity, with inhibition values below 5%. Compared to the standard compound allopurinol (IC_{50} 14.70 ± 0.71 μg/mL), the leaf essential oil demonstrated the strongest XO inhibitory activity, with an IC_{50} of 60.77 ± 2.21 μg/mL, whereas the twig and flower essential oils failed to do so (inactive, IC_{50} > 100 μg/mL) (Table 2).

The XO inhibitory effects of *Ligustrum* essential oils are first evaluated in this research. In traditional Chinese medicine, *L. lucidum* fruits, locally named Nuzhenzi, are commonly used as a tonic for the kidneys and liver [12]. Its 95% ethanol extract inhibited the XO enzyme with an IC_{50} value of 7.54 mg/mL [12]. The XO inhibitory activities of *L. lucidum* fruits, collected from Hubei and Yunnan, China, are better than those from other areas [13]. Further research on this topic using *Ligustrum* constituents is anticipated.

2.2.3 | Anti-Inflammatory Activity

The cytotoxicity of the studied essential oils toward RAW 264.7 cells was assessed at various concentrations of 4–256 μg/mL. *L. sinense* twig essential oil possessed the highest cell viability, ranging from 95 ± 2.1 at 256 μg/mL to 100% at lower concentrations (Figure 2). The leaf essential oil caused high viability levels, ranging from 92 ± 2.3 to 100%. In contrast, the flower essential oil showed a greater cytotoxic effect, as indicated by a decrease in cell viability to 82% ± 2.5% at 256 μg/mL.

TABLE 2 | The IC_{50} values (μg/mL) in the biological activities of *Ligustrum sinense* essential oils.

Samples	DPPH radical scavenging	XO inhibition	NO inhibition	α-Glucosidase inhibition	PTP1B inhibition
Twigs	201.64 ± 0.05	>100	137.85 ± 8.09	245.39 ± 4.64	225.16 ± 3.89
Leaves	4.51 ± 0.03	60.77 ± 2.21	>256	208.09 ± 4.71	124.42 ± 3.83
Flowers	>512	>100	62.83 ± 2.95	235.11 ± 4.36	175.56 ± 3.61
Ascorbic acid	13.64 ± 0.02				
Allopurinol		14.70 ± 0.71			
L-NMMA			11.00 ± 0.80		
Acarbose				241.76 ± 2.66	
Ursolic acid					46.97 ± 2.89

Abbreviations: L-NMMA, N^G-monomethyl-L-arginine acetate; NO, nitric oxide; PTP1B, protein tyrosine phosphatase 1B; XO, xanthine oxidase.

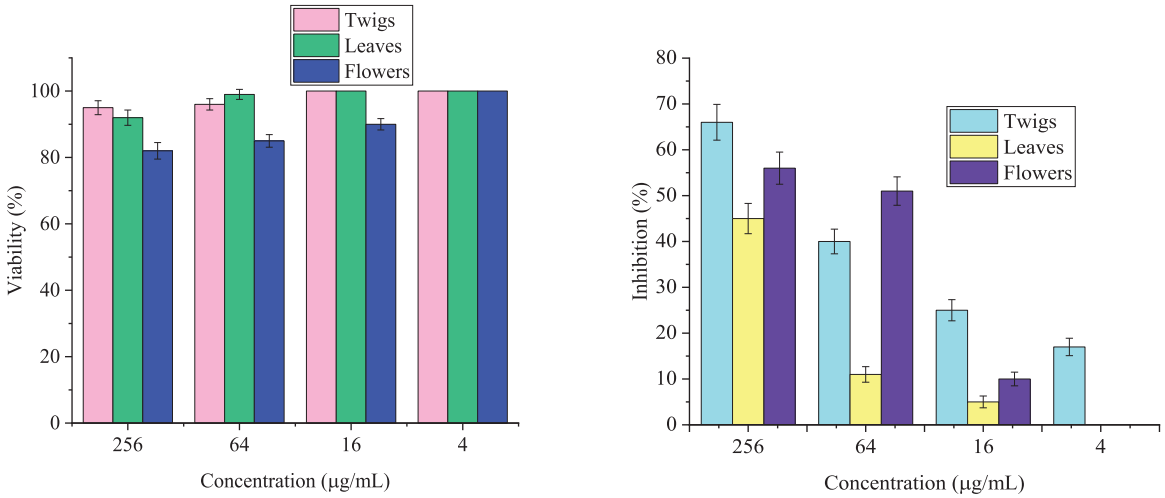

FIGURE 2 | The NO inhibition of *Ligustrum sinense* essential oils. Mean ± SD, n value = 3, $p < 0.05$ versus the non-treated group (0% inhibition).

iNOS				
COX-2				
GAPDH	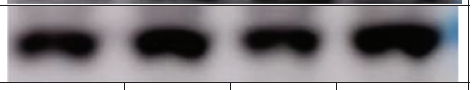			
LPS (1 μg/mL)	-	+	+	+
Essential oil	-	30	60	120

FIGURE 3 | The western blot analysis for the iNOS and COX-2 expressions in the absence/presence of *Ligustrum sinense* flower essential oils (30, 60, and 120 μg/mL). COX-2, cyclooxygenase-2; iNOS, inducible nitric oxide synthase; LPS, lipopolysaccharide.

The nitric oxide (NO) inhibition was found to be concentration-dependent for all essential oils (Figure 2). Among them, the flower essential oil exhibited the most potency, achieving 56% ± 3.5% inhibition at 256 μg/mL with an IC_{50} value of 62.83 ± 2.95 μg/mL, when L-NMMA was used as a standard (IC_{50} 11.00 ± 0.80 μg/mL). The twig sample also showed good activity, reaching 66% ± 3.9% inhibition at the same concentration, but with a higher IC_{50} of 137.85 ± 8.09 μg/mL, indicating lower potency. In contrast, the leaf essential oil showed weak activity, with a maximum inhibition of 45% ± 3.3% at 256 μg/mL and no detectable IC_{50} value within the tested range (IC_{50} >256 μg/mL). The superior NO inhibitory activity of *L. sinense* flower and twig essential oils may be attributed to their higher content of sesquiterpene hydrocarbons and oxygenated diterpenes, especially the role of the major compound *cis*-phytol.

L. sinense flower essential oil has been further considered for inhibiting the prostaglandin E2 (PGE2) release and expression of inducible nitric oxide synthase (iNOS) and cyclooxygenase 2 (COX-2). Compared to the (+) lipopolysaccharide (LPS) group, the PGE2 amount was found to be decreased in the use of 30, 60, and 120 μg/mL of essential oil (Table 3). The studied essential oil also reduced the expression of inflammatory proteins at 120 μg/mL (Table 3 and Figure 3).

For the first time, the inflammatory potency of *Ligustrum* essential oil has been documented. The current study aligns with previous records because *Ligustrum* constituents are appropriate for inflammatory treatments. At 0.05–0.2 mg/mL, the ethanol extract of *Ligustrum ovalifolium* leaves could reduce the NO and reactive oxygen species (ROS) production and iNOS and COX-2 expressions [14]. The methanol extracts of *L. lucidum* and *Ligustrum pricei* aerial parts showed in vivo inflammatory activity in carrageenan-induced edema in rodents [4]. At 25 μM, ligureside B, a new iridoid glycoside from *L. lucidum* fruits, showed 22.10% inhibition against NO production, compared to that of the standard indomethacin (45.08%) [15].

2.2.4 | α-Glucosidase Inhibitory Activity

The α-glucosidase inhibitory activity of essential oils from *L. sinense* twigs, leaves, and flowers was assessed at various concentrations of 32–512 μg/mL (Table 2 and Figure 4). All the studied samples exhibited a dose-dependent inhibition with varying potencies. At 512 μg/mL, the leaf essential oil showed the highest inhibition of 79.49% ± 1.50%, followed by the flower essential oil (76.85% ± 1.55%) and the twig essential oil (75.73% ± 1.60%). The trend was consistent with lower concentrations. At 256 μg/mL, the inhibition levels were 57.74% ± 2.00% (leaves), 54.35% ± 2.05% (flowers), and 52.95% ± 2.10% (twigs). At 128 μg/mL, they decreased to 36.63% ± 2.50%, 33.65% ± 2.55%, and 32.63% ± 2.60% for the leaves, flowers, and twigs, respectively. At the lowest tested concentration of 32 μg/mL, the inhibition remained about 9%–10%.

As a result, IC_{50} values confirmed the rank order of activity: the leaf essential oil (IC_{50} 208.09 ± 4.71 μg/mL) > the flower essential oil (IC_{50} 235.11 ± 4.36 μg/mL) > acarbose (IC_{50} 241.76 ± 2.66 μg/mL) > the twig essential oil (IC_{50} 245.39 ± 4.64 μg/mL). These findings highlight the α-glucosidase inhibitory potencies of *L. sinense* essential oils, which may be attributed to their relatively high levels of major compounds.

Ligustrum essential oils are first evaluated for α-glucosidase inhibitory activities in this study. The results are in line with the

TABLE 3 | The PGE2 amount and the levels of iNOS and COX-2 expression at the tested concentrations of *Ligustrum sinense* flower essential oil.

PGE2 amount (pg/mL)			
Essential oil	30 μg/mL	60 μg/mL	120 μg/mL
	3309.68 ± 87.32	3103.17 ± 111.63	3044.65* ± 91.12
Celecoxib (20 μM)		1482.26** ± 67.48	
(+) LPS (1 μg/mL)		3365.19 ± 122.47	
(−) LPS		621.13 ± 21.47	
iNOS and COX-2 levels (pg/mL)			
Essential oil	30 μg/mL	60 μg/mL	120 μg/mL
iNOS	1.03	1.16	0.88
COX-2	1.06	0.81	0.64*
LPS (1 μg/mL)		1	

Abbreviations: COX-2, cyclooxygenase-2; iNOS, inducible nitric oxide synthase; LPS, lipopolysaccharide; PGE2, prostagladin E2.
*$p < 0.05$ versus the (+) LPS group.
**$p < 0.01$ versus the (+) LPS group.

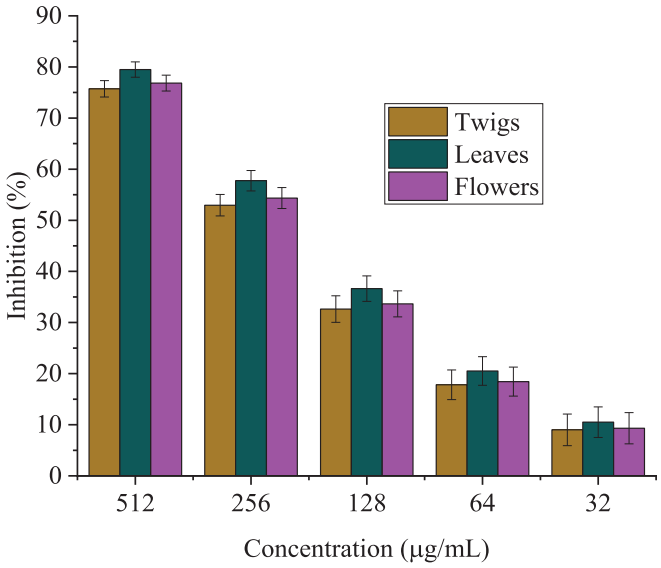

FIGURE 4 | The α-glucosidase inhibition of *Ligustrum sinense* essential oils. Mean ± SD, n value = 3, $p < 0.05$ versus the non-treated group (0% inhibition).

findings of earlier reports, in which *Ligustrum* constituents are also recommended for anti-diabetes. *trans-p*-Hydroxycinnamic acid, a phenolic compound isolated from the 70% ethanol extract of *L. robustum* leaves, showed stronger α-glucosidase inhibition (IC_{50} 1.15 ± 0.08 nM) than acarbose (IC_{50} 5.50 ± 0.11 nM) [16]. A triterpenoid was separated from *L. lucidum*, namely, oleanolic acid, which could inhibit alloxan-induced diabetic rats at 60 and 100 mg/kg [17].

2.2.5 | Protein Tyrosine Phosphatase 1B (PTP1B) Inhibitory Activity

The PTP1B inhibitory activity of *L. sinense* essential oils was evaluated at various concentrations of 32–512 μg/mL. All three samples exhibited a dose-dependent inhibition pattern with varying potencies. At the highest tested concentration of 512 μg/mL, the leaf essential oil exerted the strongest inhibition at 90.03% ± 1.20%, followed by the flower sample (85.05% ± 1.30%) and twig sample (80.49% ± 1.40%). This trend persisted across lower concentrations, with the inhibitions decreasing accordingly. At 256 μg/mL, essential oils from the leaves, flowers, and twigs exhibited inhibitory percentages of 75.08 ± 1.70, 67.48 ± 1.80, and 59.08 ± 1.90, respectively. At the lowest tested concentration of 32 μg/mL, the inhibitions remained measurable from 10% to 15% (Figure S5). As a consequence, the leaf essential oil was the most active with an IC_{50} of 124.42 ± 3.83 μg/mL, followed by the flower essential oil (IC_{50} 175.56 ± 3.61 μg/mL) and twig essential oil (IC_{50} 225.16 ± 3.89 μg/mL) (Table 2). Compared to the standard ursolic acid (IC_{50} 46.97 ± 2.89 μg/mL), all essential oils had lower inhibitory action.

2.2.6 | Antimicrobial Activity

L. sinense essential oils possessed varying degrees of activity against *Staphylococcus aureus* and *Candida albicans*, with a clear dependence on both concentration and plant part (Table 4). The leaf essential oil exhibited the most significant inhibition zones (IZs) against *S. aureus*, increasing from 14.90 ± 1.06 mm (50 μg/mL) to 19.07 ± 0.50 mm (200 μg/mL), followed by the flower essential oil (IZ 13.90–15.50 mm). In contrast, the twig essential oil was inactive at lower concentrations and only weakly active at 200 μg/mL (IZ 9.70 ± 0.49 mm). Regarding *C. albicans*, a similar pattern was observed: The flower and leaf essential oils displayed moderate activity (up to 13.53 ± 0.51 and 13.17 ± 0.49 mm at 200 μg/mL, respectively), whereas twig essential oil again showed weak inhibition. Compared to the standard ampicillin (IZs > 30 mm), the studied essential oils were substantially less potent.

From Table 1, the superior antimicrobial activity observed in the leaf and flower essential oils compared to the twig essential oil can be attributed to their higher content of sesquiterpene hydrocarbons. Both leaf and flower oils also contained significant

TABLE 4 | The zone of inhibition (ZI) of the studied essential oils in the antimicrobial assay.

Samples	*Staphylococcus aureus*			*Candida albicans*		
	50 μg/mL	100 μg/mL	200 μg/mL	50 μg/mL	100 μg/mL	200 μg/mL
Ligustrum sinense leaves	14.90 ± 1.06	17.30 ± 1.18	19.07 ± 0.50	8.00 ± 0.65	12.42 ± 0.65	13.17 ± 0.49
L. sinense twigs	Inactive	Inactive	9.70 ± 0.49	Inactive	10.12 ± 0.37	9.10 ± 0.50
L. sinense flowers	13.90 ± 0.83	15.30 ± 0.67	15.50 ± 0.31	9.51 ± 0.73	10.16 ± 0.35	13.53 ± 0.51
Ampicillin (10 μg/mL)	31.70 ± 0.99	30.80 ± 1.77	32.20 ± 0.40	31.70 ± 0.09	31.45 ± 0.15	31.10 ± 0.80

amounts of linalool (7.4% and 6.9%, respectively) and germacrene B (14.2% and 17.2%, respectively), terpenoids known for their antimicrobial effects. In contrast, the twig essential oil contained a higher proportion of non-terpenic and hydrocarbon constituents, which likely contributes to its weaker antimicrobial activity. These findings are consistent with previous studies reporting the antimicrobial effects of *Ligustrum* species.

At 1 mg/dics, *L. lucidum* flower essential oil could suppress the growth of microbial strains *Bacillus subtilis*, *Escherichia coli*, *Listeria monocytogenes*, *Salmonella enterica*, and *S. aureus*, with IZs ranging from 14.62 to 19.66 mm [10]. Antibacterial action of *L. obtusifolium* flower essential oil could be explained by altering membrane permeability parameters [8]. Linalool isolated from *L. compactum* flower essential oil was responsible for antibacterial activity against *Pseudomonas aeruginosa* (IZ 18.5 ± 0.7 mm) and *Shigella sonnei* (IZ 18.9 ± 1.2 mm) [9]. These findings suggest that *Ligustrum* essential oils could serve as supplementary or alternative options for managing bacterial infections, especially in the context of increasing antibiotic resistance.

2.3 | Molecular Docking

Molecular docking simulations were carried out on four major essential oil compounds—linalool, methyl salicylate, germacrene B, and *cis*-phytol—to explore their antidiabetic potential. These metabolites are presumed to contribute significantly to the antidiabetic and other biological activities of the investigated essential oils. The selection strategy aimed to investigate the molecular interactions between these major constituents and the human aldose reductase (PDB ID: 3WY1), a key enzyme involved in the polyol pathway of glucose metabolism, where it could catalyze the reduction of glucose to sorbitol [18]. Under conditions of hyperglycemia, the overactivation of aldose reductase plays a great role in diabetic pathogenesis. By this, aldose reductase has emerged as a validated pharmacological target for therapeutic intervention in diabetes-associated disorders. The crystal structure of the enzyme (PDB ID: 3WY1) at a high resolution of 1.27 Å, complexed with a specific inhibitor, enables detailed characterization of the active site, thus offering a valuable framework for structure-based drug design and virtual screening of potential inhibitors [19].

Among the tested molecules, germacrene B exhibited the most favorable binding energy (−6.637 kcal/mol), primarily through hydrophobic interactions involving Ala349, Lys352, His515, and Phe516 (Figure 5 and Table 5). These residues were located near the enzyme's hydrophobic binding groove, suggesting a stable accommodation of the ligand. *cis*-Phytol also demonstrated a comparatively strong binding affinity (−5.729 kcal/mol) and was stabilized via multiple alkyl and π–alkyl interactions with amino acid residues Ala451, Ala454, Ala444, His348, Leu433, His515, Pro442, and Arg450. The abundance of nonpolar contacts indicated the predominance of hydrophobic forces in the binding process. Methyl salicylate, with a docking energy of −5.233 kcal/mol, formed a key hydrogen bond with Arg437, alongside additional π–alkyl contacts (with residues Ala444 and Ala454) and a carbon–hydrogen bond with Glu432 (Figure 5 and Table 5). Significantly, the involvement of Arg437, a residue also implicated in the binding of the reference inhibitor acarbose, suggested a possible shared mode of inhibition. Linalool showed the lowest binding affinity (−5.174 kcal/mol) but remained engaged through hydrophobic interactions with Leu433, Ala444, and His348. Despite the absence of polar contacts, its docking profile supported a moderate interaction potential within the enzyme's active site. Collectively, these findings indicated that certain essential oil constituents may exert antidiabetic activity through specific hydrophobic or hydrogen bonding interactions and thus represent promising scaffolds for the development of plant-derived antidiabetic agents.

2.4 | Toxicity Prediction

Toxicity predictions of these major compounds revealed differential organ-specific toxicological profiles (Figure S6 and Table S1). Methyl salicylate exhibited active hepatotoxicity (0.55) and nephrotoxicity (0.71), indicating a potential risk of liver and kidney damage upon prolonged exposure, despite being inactive in neurotoxicity and respiratory toxicity. In contrast, *cis*-phytol, germacrene B, and linalool were predicted to be inactive across all tested toxicity categories, suggesting a relatively safer toxicological profile. In addition to organ toxicity, the acute toxicity was assessed on the basis of LD_{50} values and corresponding toxicity classes. Methyl salicylate showed the lowest LD_{50} value (887 mg/kg), falling into toxicity class 4, indicating it is slightly toxic. Meanwhile, *cis*-phytol (LD_{50} 5000 mg/kg), germacrene B (LD_{50} 4390 mg/kg), and linalool (LD_{50} 2200 mg/kg) belonged to toxicity class 5, reflecting a lower level of acute toxicity. These findings are particularly relevant in a molecular docking analysis, as the selected compounds demonstrated favorable binding interactions with the α-glucosidase enzyme. The combination of high binding affinity and low predicted toxicity, especially for *cis*-phytol and linalool, supports their potential as promising lead candidates for further development as diabetic inhibitors.

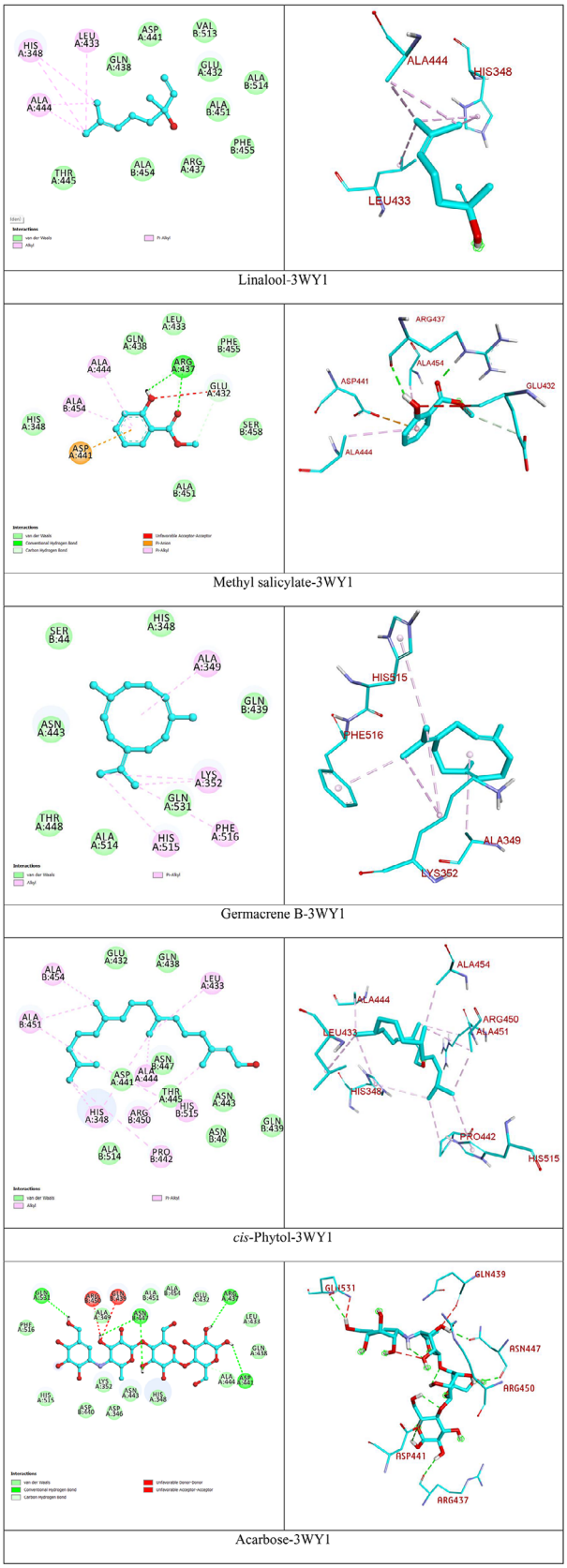

FIGURE 5 | The 2D and 3D interaction profiles of the major compounds and protein 3WY1.

3 | Conclusions

The current research fully provides chemical profiles of essential oils from *L. sinense* twigs, leaves, and flowers. By the GC–MS analysis, the main classes have been documented to include oxygenated monoterpenes, sesquiterpene hydrocarbons, oxygenated sesquiterpenes, and non-terpenic compounds. Linalool, methyl salicylate, germacrene B, and *cis*-phytol are likely to be the major compounds. *L. sinense* essential oils exhibited a broad panel of biological activities, including antioxidant, anti-gout, anti-inflammation, anti-diabetes, and antimicrobial activity. In addition, molecular docking simulations supported the α-glucosidase inhibitory capacity of these compounds, particularly germacrene B and *cis*-phytol, which showed strong binding affinities and favorable safety predictions. These findings suggest that *L. sinense* essential oils are a promising source of bioactive molecules for metabolic disorder treatments. However, the current body of research remains limited, and further studies are needed to fully characterize their bioactive compounds, mechanisms of action, and experimental safety profiles. Future investigations should also focus on elucidating the possible synergistic or antagonistic interactions among the constituents, which may underlie the overall biological effects of the essential oils.

4 | Materials and Methods

4.1 | Plant Materials

The fresh twigs, leaves, and flowers were collected from A Luoi, Thua Thien Hue, Vietnam, at 16°22′33.8″ N and 107°34′06.9″ E on March 3, 2025. The botanical name was confirmed by co-author Dr. Nguyen Thi Kim Thanh, University of Science, VNU. The voucher specimens LST-2024 (twigs), LSL-2024 (leaves), and LSF-2024 (flowers) were deposited in Hue University.

4.2 | Hydro-Distilled Procedure

The fresh powdered material (1.5 kg) of each plant part was subjected to hydro-distillation with 3.0 L of deionized water using a Clevenger-type apparatus at 100°C for 2.6 h. The resulting distillate was extracted three times with *n*-hexane. The combined organic layers were dried over anhydrous Na_2SO_4, filtered, and subsequently concentrated under decreased pressure to discard the solvent. The obtained essential oils were stored at 4°C until further analysis. On the basis of fresh weight, the extraction yields of 0.34%, 0.37%, and 0.26% v/w were assigned for the twigs, leaves, and flowers, respectively.

4.3 | GC–MS Analysis

Chemical compositions in *L. sinense* essential oils were analyzed using a Shimadzu GC–MS-QP2010 Plus system (Shimadzu, Kyoto, Japan) equipped with a fused silica Equity-5 capillary column (30 m × 0.25 mm i.d., film thickness 0.25 μm; Supelco, USA) [20]. Helium was used as the carrier gas at a constant flow rate of 1.5 mL/min. The injector and interface temperatures were both set at 260°C. The oven temperature was initially held at 45°C for 2.0 min, ramped to 240°C at 4°C/min (held for 10 min), then

TABLE 5 | Binding affinities and molecular interactions of selected essential oil compounds with the human aldose reductase enzyme.

Compounds	Binding affinity (kcal/mol)	Interaction type	Interacting amino acid residues
Linalool	−5.174	Alkyl; π–alkyl	Leu433, Ala444, and His348
Methyl salicylate	−5.233	Hydrogen bond	Arg437
		π–Alkyl	Ala444, and Ala454
		Carbon–hydrogen bond	Glu432
Germacrene B	−6.637	Alkyl; π–alkyl	Ala349, Lys352, His515, and Phe516
cis-Phytol	−5.729	Alkyl; π–alkyl	Ala451, Ala454, Ala444, His348, Leu433, His515, Pro442, and Arg450
Acarbose	−9.486	Hydrogen bond	Arg437, Asp441, Asn447, and Gln531

increased to 260°C at 5°C/min and held for a further 9 min. The injection was performed in split mode with a ratio of 10:1, an inlet pressure of 93.2 kPa, and an injection volume of 1.2 μL.

MS conditions included electron ionization (EI) at 70 eV, a detector voltage of 0.82 kV, and a scan range of *m/z* 45–550, with a sampling rate of 0.5 scan/s. Retention indices (RIs) were calculated on the basis of the retention times of a homologous series of *n*-alkanes C7–C40 run under identical conditions. The identification of the chemical compounds was carried out by comparing the calculated RIs and mass spectra with data from literature and by referencing the NIST 11 and WILEY 7 mass spectral libraries. Quantification of the volatile constituents was based on the relative peak areas obtained from the total ion chromatograms (TICs).

4.4 | Biological Assays

4.4.1 | Antioxidative Assay

The antioxidant activity of essential oils was assessed using the DPPH radical scavenging assay [21]. A DPPH solution (0.15 mM) in ethanol (200 μL) was mixed with 1.4 μL of essential oil dissolved in DMSO (with the final concentrations of 32–512 μg/mL) in a 96-well microplate. The mixture was then incubated at 25°C for 30 min, and the absorbance was recorded at 517 nm using a UV–Vis spectrophotometer. Inhibition (%) was determined using the standard formula:

$$\text{Inhibition}\,(\%) = [(A_{\text{control}} - A_{\text{sample}})/A_{\text{control}}] \times 100$$

where A_{control} and A_{sample} were the absorbance of the control (without inhibitor) and absorbance in the presence of essential oil, respectively. The assay was repeatedly performed three times. Ascorbic acid at the concentrations of 0.1–10 μg/mL was used as a positive control. IC_{50} values were obtained using Microsoft Excel.

4.4.2 | XO Assay

The XO inhibitory assay was carried out following previous reports with several modifications [22]. A reaction mixture contained 50 μL of essential oil, 35 μL of 70 mM phosphate buffer (pH 7.5), and 30 μL of the XO enzyme solution (0.01 U/mL in the same buffer). After preincubation at 25°C for 15 min, the reaction was initiated by adding 60 μL of 150 mM xanthine substrate in phosphate buffer. The mixture was then incubated at 25°C for 30 min. The reaction was furnished by adding 25 μL of 1 N HCl, and the absorbance was recorded at 290 nm using an ELISA microplate reader. The assay was repeatedly performed three times. Allopurinol at the concentrations of 0.1–10 μg/mL was used as a positive control. IC_{50} values were obtained using Microsoft Excel.

4.5 | Anti-Inflammatory Assay

4.5.1 | NO Inhibitory Assay

RAW 264.7 cells (ATCC TIB-71) were cultured in Dulbecco's Modified Eagle's Medium (DMEM) supplemented with 10% fetal bovine serum (FBS) and 1% antibiotic–antimycotic (Gibco) at 37°C in a humidified atmosphere containing 5% CO_2 [23]. RAW 264.7 cells were seeded into 96-well microplates at 2×10^5 cells/well and incubated at 37°C in 5% CO_2 for 24 h. The culture medium was then replaced with serum-free DMEM and incubated for 3 h. Following serum starvation, cells were treated with essential oil (4–256 μg/mL) for 2 h, followed by stimulation with LPS (1 μg/mL) for 24 h to induce NO production.

Nitrite (NO_2^-), a stable end product of NO, was measured using the Griess reagent. Briefly, 100 μL of culture supernatant was transferred to a new 96-well microplate and mixed with 100 μL of Griess reagent. The mixture was incubated at 25°C for 10 min, and the NO_2^- levels were determined spectrophotometrically at 540 nm. Wells containing only the culture medium served as the negative control. N^G-Methyl-L-arginine acetate (L-NMMA) at the concentrations of 0.1–10 μg/mL was used as a positive control. IC_{50} values were obtained using Microsoft Excel.

4.5.2 | PGE2 Inhibitory Assay

RAW 264.7 cells were seeded into 96-well microplates at 5×10^4 cells/well and incubated at 37°C in 5% CO_2 for 24 h. *L. sinense*

flower essential oil (30–120 μg/mL) of 10 μL was then added [24]. The control wells (+LPS) contained cells and 10% DMSO, without the tested sample, whereas wells containing only the culture medium served as the negative control. For 2 h of pre-treatment, LPS (1 μg/mL) was added to the experimental wells. The negative control (−LPS) did not contain LPS, to assess the basal expression of PGE2. After 24 h of treatment, supernatants were collected, and PGE2 levels were quantified using a Mouse PGE2 ELISA Kit (R&D Systems, Minneapolis, USA).

4.5.3 | Western Blot Analysis

RAW 264.7 cells were seeded into 96-well microplates at 2×10^6 cells/well and incubated at 37°C in 5% CO_2 for 24 h. Subsequently, the cells were treated with *L. sinense* flower essential oil (30–120 μg/mL) in a medium stimulated by LPS (1 μg/mL) for 24 h [24]. After treatment, the cells were washed twice with cold PBS and lysed using RIPA buffer containing a protease inhibitory cocktail (Promega). The lysates were centrifuged at 12 000 rpm for 10 min at 4°C, and the supernatants were gathered. Total protein concentration was determined using the Bradford assay. For each sample, 30 μg of protein was mixed with loading buffer (Bio-Rad) and β-mercaptoethanol (Sigma-Aldrich, USA), then denatured at 95°C for 5 min.

Proteins were separated on 12% SDS–PAGE gels (Bio-Rad), electrophoresed at 90 V for the first 10 min, followed by 120 V for 90 min. The gels were transferred onto PVDF membranes (Bio-Rad) using a transfer buffer (192 mM glycine, 25 mM Tris, 1% SDS, 20% ethanol) at 28 V for 30 min at 4°C. After transfer, the PVDF membranes were blocked with TBS containing 5% BSA and then incubated overnight at 4°C with primary antibodies: anti-iNOS and anti-COX-2 (Prointech). Following washes, the membranes were incubated with secondary antibodies (anti-rabbit IgG for iNOS and anti-mouse IgG for COX-2) for 1 h at 25°C. Protein bands were visualized using ECL detection reagents and imaged with an Azure Biosystems C300 imaging system. Band intensities were analyzed using the ImageJ software (https://imagej.nih.gov/ij/) and normalized to the LPS-positive control. Glyceraldehyde 3-phosphate dehydrogenase (GAPDH) was used as an internal loading control to normalize the loaded protein amount and to accurately evaluate the relative expression levels of iNOS and COX-2 proteins.

4.5.4 | α-Glucosidase Inhibitory Assay

The assay was performed following previously reported protocols [25]. Serial concentrations of essential oil (32–512 μg/mL) were prepared by dissolving the samples in DMSO (400 mg/mL). The reaction mixture, consisting of the sample solution, phosphate buffer (100 mM, pH 6.8), and α-glucosidase enzyme (0.4 U/mL), was preincubated in 96-well microplates at 37°C for 10 min. Subsequently, *p*-nitrophenyl-β-D-glucopyranoside (pNPG, 2.5 mM) was added to initiate the reaction. The mixture was further incubated at 37°C for 30 min, after which the reaction was terminated by adding sodium carbonate (0.2 M). The amount of *p*-nitrophenol released, indicated by the formation of a yellow color, was measured at 410 nm using an ELISA microplate reader. Acarbose at the concentrations of 0.1–10 μg/mL was used as a positive control. IC_{50} values were obtained using Microsoft Excel.

4.5.5 | PTP1B Inhibitory Assay

PTP1B (human, recombinant) was obtained from BIOMOL International LP (USA), and its enzymatic activity was evaluated using *p*-nitrophenyl phosphate (*p*-NPP) as the substrate, following the method described by Hung et al. [26]. In each well of a 96-well microplate (final volume: 200 μL), a reaction mixture containing 2 mM *p*-NPP and PTP1B (0.05–0.1 μg) was prepared in a buffer composed of 50 mM citrate (pH 6.0), 0.1 M NaCl, 1 mM EDTA, and 1 mM dithiothreitol (DTT), with or without essential oil samples. After incubation at 37°C for 30 min, the reaction was terminated by the addition of 10 M NaOH. The amount of *p*-nitrophenol produced was quantified by measuring the absorbance at 405 nm. Ursolic acid at the concentrations of 0.1–10 μg/mL was used as a positive control. IC_{50} values were obtained using Microsoft Excel.

4.5.6 | Antimicrobial Assay

The antimicrobial activity of essential oils was evaluated using the agar well diffusion method and assessed on the basis of the diameter of the IZs [27]. The microbial strains included the Gram (+) bacterium *S. aureus* ATCC 25923 and the yeast *C. albicans* ATCC 10231. A 0.1 mL aliquot of the test bacterial suspension, with a density of 10^6 CFU/mL, was evenly spread onto the surface of Petri dishes containing tryptic soy broth (TSB) agar and allowed to dry. Sterile cork borers were then used to punch wells with a diameter of 6 mm into the agar. Subsequently, 50 μL of essential oil (50–200 μg/mL) was introduced into each well. The tested plates were incubated for 24 h, after which antimicrobial activity was evaluated by observing and recording IZs. Ampicillin (10 μg/mL) and 10% DMSO were used as positive and negative controls, respectively.

4.6 | Statistical Analysis

Data were analyzed using the Origin 2025 Release Notes and expressed as mean ± SD (standard deviation). The statistical difference was meaningful with $p < 0.05$.

4.6.1 | Computational Procedure

The three-dimensional (3D) structure of the α-glucosidase enzyme was obtained from the RCSB Protein Data Bank (PDB ID: 3WY1) [19]. Before molecular docking, the protein structure was prepared using AutoDockTools v1.5.6 by removing co-crystallized water molecules, adding missing polar hydrogens, and assigning Kollman charges to all atoms. The 3D structures of the major essential oil compounds were constructed and energy-minimized using Chem3D with the MM2 force field. Docking simulations were then performed using the AutoDock Vina v1.2.3 program [28]. Targeted docking was conducted within the enzyme's active site using a grid box centered at coordinates $x = 3.391$ Å, $y = 1.310$ Å, and $z = -8.362$ Å, with dimensions of 24 × 24 × 24 points and a grid spacing of 1 Å. Other parameters were kept at

the default. Binding affinities were recorded in kcal/mol. Protein–ligand interactions were visualized and interpreted using BIOVIA Discovery Studio Visualizer. In addition, the toxicological profiles of the docked compounds were predicted via the pkCSM web server [29].

Author Contributions

Ninh The Son: supervision, writing – review and editing. **Phan Hong Minh**: formal analysis. **Huynh Thi Ngoc Ni**: validation. **Nguyen Ngoc Linh**: validation. **Nguyen Thi Kim Thanh**: resources. **Le The Hoai**: investigation. **Nguyen Thi Thoa**: investigation. **Nguyen Xuan Ha**: investigation. **Ty Viet Pham**: conceptualization. All authors have read and approved the finalized manuscript.

Funding

The authors have nothing to report.

Conflicts of Interest

The authors declare no conflicts of interest.

Data Availability Statement

The data that support the findings of this study are available in the Supporting Information section of this article.

References

1. J. L. Hanula, S. Horn, and J. W. Taylor, "Chinese Privet (*Ligustrum sinense*) Removal and Its Effect on Native Plant Communities of Riparian Forests," *Invasive Plant Science and Management* 2 (2009): 292–300, https://doi.org/10.1614/IPSM-09-028.1.

2. Y. Liu, D. X. Lu, J. Huang, et al., "Aromatic Glycosides From the Aerial Part of *Bupleurum chinense*," *Journal of Asian Natural Products Research* 24 (2022): 1078–1085, https://doi.org/10.1080/10286020.2021.2017897.

3. T. A. Nong, H. L. Lo, A. H. Dao, et al., "Neolignan Glycoside and Other Constituents From the Leaves of *Ligustrum sinense* and Their Anti-Inflammatory Activity," *Natural Products Communications* 19 (2024): 1–5, https://doi.org/10.1177/1934578X241226825.

4. C. R. Wu, Y. C. Hseu, J. C. Lien, L. W. Lin, Y. T. Lin, and H. Ching, "Triterpenoid Contents and Anti-Inflammatory Properties of the Methanol Extracts of *Ligustrum* Species Leaves," *Molecules (Basel, Switzerland)* 16 (2011): 1–15, https://doi.org/10.3390/molecules16010001.

5. D. M. Yang, M. A. Quyang, and S. Q. Lv, "Combined Treatment of *Pseudomonas aeruginosa* PA01 Biofilm Formation With the Water Soluble Extract of *Ligustrum sinense* and Gentamicin Sulphate," *Journal of Environmental Biology* 34 (2013): 451–457.

6. H. S. Lee, "Chemical Composition and Acaricidal Effects of Essential Oils Extracted From *Ligustrum japonicum* Against Acaridae and Pyroglyphid Mites," *Journal of Applied Biological Chemistry* 58 (2015): 197–199, https://doi.org/10.3839/jabc.2015.031.

7. H. W. Wu, L. Y. Zhao, Y. T. Zheng, T. Xiang, and Y. Li, "Analysis of Chemical Components of Volatile Oils From Small Leaves *Ligustrum robust*," *Medicinal plants* 3 (2012): 37–39.

8. P. Bhalla and V. K. Bajpai, "Antibacterial Mechanistic Effects of Flower Essential Oil of *Ligustrum obtusifolium* Through Altering Membrane Permeability Parameters," *Journal of Essential Oil-Bearing Plants* 20 (2017): 380–387, https://doi.org/10.1080/0972060X.2017.1325333.

9. L. Yu, J. X. Ren, H. M. Nan, and B. F. Liu, "Identification of Antibacterial and Antioxidant Constituents of the Essential Oils of *Cynanchum chinense* and *Ligustrum compactum*," *Natural Product Research* 29 (2015): 1779–1782, https://doi.org/10.1080/14786419.2014.1000322.

10. V. K. Bajpai, S. Singh, and A. Mehta, "Chemical Characterization and Mode of Action of *Ligustrum lucidum* Flower Essential Oil Against Food Borne Pathogenic Bacteria," *Bangladesh Journal of Pharmacology* 11 (2016): 269–280, https://doi.org/10.3329/bjp.v11i1.25487.

11. K. M. Lau, Z. D. He, H. Dong, K. P. Fung, and P. P. H. But, "Anti-Oxidative, Anti-Inflammatory and Hepatoprotective Effects of *Ligustrum robustum*," *Journal of Ethnopharmacology* 83 (2002): 63–71, https://doi.org/10.1016/S0378-8741(02)00192-7.

12. H. M. Lin, F. L. Yen, L. T. Ng, and C. C. Lin, "Protective Effects of *Ligustrum lucidum* Fruit Extract on Acute Butylated Hydroxytoluene Induced Oxidative Stress in Rats," *Journal of Ethnopharmacology* 111 (2007): 129–136, https://doi.org/10.1016/j.jep.2006.11.004.

13. S. Gao, H. Chen, and X. Zhou, "Study on the Spectrum-Effect Relationship of the Xanthine Oxidase Inhibitory Activity of *Ligustrum lucidum*," *Journal of Separation Science* 42 (2019): 2834–2844, https://doi.org/10.1002/jssc.201900531.

14. M. Y. Lee, I. S. Shin, H. S. Lim, and H. K. Shin, "Anti-Inflammatory Effects of Extracts From *Ligustrum ovalifolium* H. Leaves on RAW264.7 Macrophages," *Journal of the Korean Society of Food Science and Nutrition* 41 (2012): 1205–1211, https://doi.org/10.3746/jkfn.2012.41.9.1205.

15. N. Zengin, A. Mollica, D. Stefanucci, et al., "Multidirectional Biological Evaluation and Chemical Profiling of *Ligustrum lucidum* W.T.Aiton: A Source of Functional Biomolecules for Novel Nutraceutical and Cosmeceutical Applications," *Fitoterapia* 169 (2023): 105705, https://doi.org/10.1016/j.fitote.2023.105705.

16. S. H. Lu, H. J. Zuo, J. X. Shi, et al., "Two New Glycosides From the Leaves of *Ligustrum robustum* and Their Antioxidant Activities and Inhibitory Effects on α-Glucosidase and α-Amylase," *South African Journal of Botany* 125 (2019): 521–526, https://doi.org/10.1016/j.sajb.2019.07.028.

17. D. Gao, Q. Li, and Y. Li, "Antidiabetic and Antioxidant Effects of Oleanolic Acid From *Ligustrum lucidum* Ait in Alloxan-Induced Diabetic Rats," *Phytotherapy Research* 23 (2009): 1257–1262, https://doi.org/10.1002/ptr.2603.

18. M. Brownlee, "Biochemistry and Molecular Cell Biology of Diabetic Complications," *Nature* 414 (2001): 813–820, https://doi.org/10.1038/414813a.

19. X. Shen, W. Saburi, and Z. Gai, "Structural Analysis of the α-Glucosidase HaG Provides New Insights Into Substrate Specificity and Catalytic Mechanism," *Acta Crystallographica Section D, Biological Crystallography* 71 (2015): 1382–1391, https://doi.org/10.1107/S139900471500721X.

20. Y. T. Van, D. Dinh, and D. M. Tran, "The Antimicrobial Activity and Essential Oil Constituents of the Leaves and Trunks of *Aquilaria banaensis* P. H. Hô (Thymelaeceae) From Vietnam," *Natural Product Research* 38 (2024): 744–752, https://doi.org/10.1080/14786419.2023.2196624.

21. V. M. Vu, X. Ha, and N. T. Son, "Antioxidative Potential of 3-Methoxyluteolin: Density Functional Theory (DFT), Molecular Docking and Dynamics—A Combined Experimental and Computational Study," *Chemistry and Biodiversity* 22 (2025): e202402993, https://doi.org/10.1002/cbdv.202402993.

22. X. Shen, Y. Mo, J. Ren, and K. Liu, "Inhibition of Xanthine Oxidase by Copper Gallate Coordination Polymers and Its Mechanistic Study," *Journal of Molecular Structure* 1346 (2025): 142912, https://doi.org/10.1016/j.molstruc.2025.142912.

23. R. N. Raka, Z. Ding, and Y. Yuan, "Pingyin Rose Essential Oil Alleviates LPS-Induced Inflammation in RAW 264.7 Cells via the NF-κB Pathway: An Integrated In Vitro and Network Pharmacology Analysis," *BMC Complementary Medicine and Therapies* 22 (2022): 272, https://doi.org/10.1186/s12906-022-03748-1.

24. H. Lee, Z. Liu, L. Dong, et al., "Anti-Inflammatory Effects of Polyphenolic Extract From *Artemisia iwayomogi* (PDJ) on LPS-Induced RAW 264.7 Cells," *Experimental and Therapeutic Medicine* 20 (2020): 8472, https://doi.org/10.3892/etm.2020.8472.

25. T. H. Nguyen, M. Q. Pham, V. C. Pham, et al., "Cytotoxic and α-Glucosidase Inhibitory Xanthones From *Garcinia mckeaniana* Leaves and Molecular Docking Study," *Chemistry and Biodiversity* 18 (2021): e2100396, https://doi.org/10.1002/cbdv.202100396.

26. T. M. Hung, D. M. Hoang, J. C. Kim, H. S. Jang, J. S. Ahn, and B. S. Min, "Protein Tyrosine Phosphatase 1B Inhibitory Activity of Dammaranes From Vietnamese *Giao Co Lam* Tea," *Journal of Ethnopharmacology* 124 (2009): 240–245, https://doi.org/10.1016/j.jep.2009.04.027.

27. M. Balouiri, M. Sadiki, and S. K. Ibnsouda, "Methods for In Vitro Evaluating Antimicrobial Activity: A Review," *Journal of Pharmaceutical Analysis* 6 (2016): 71–79, https://doi.org/10.1016/j.jpha.2015.11.005.

28. O. Trott and A. J. Olson, "AutoDock Vina: Improving the Speed and Accuracy of Docking With a New Scoring Function, Efficient Optimization, and Multithreading," *Journal of Computational Chemistry* 31 (2010): 455–461, https://doi.org/10.1002/jcc.21334.

29. D. E. Pires, T. L. Blundell, and D. B. Ascher, "pkCSM: Predicting Small-Molecule Pharmacokinetic and Toxicity Properties Using Graph-Based Signatures," *Journal of Medicinal Chemistry* 58 (2015): 4066–4072, https://doi.org/10.1021/acs.jmedchem.5b00104.

Supporting Information

Additional supporting information can be found online in the Supporting Information section.

Supporting File 1: cbdv70766-sup-0001-SuppMat.pdf